

# A Novel Synthetic Toehold Switch for MicroRNA Detection in Mammalian Cells

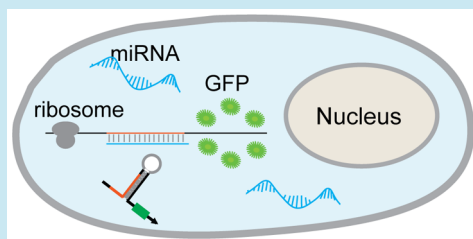
Shue Wang,<sup>†,‡</sup> Nicholas J. Emery,<sup>†,§</sup> and Allen P. Liu<sup>\*,†,‡,§,||</sup>

<sup>†</sup>Department of Mechanical Engineering, <sup>‡</sup>Department of Biomedical Engineering, <sup>§</sup>Cellular and Molecular Biology Program, <sup>||</sup>Biophysics Program, University of Michigan, Ann Arbor, Michigan 48109, United States

 Supporting Information

**ABSTRACT:** MicroRNAs (miRNA or miR) are short noncoding RNA of about 21–23 nucleotides that play critical roles in multiple aspects of biological processes by mediating translational repression through targeting messenger RNA (mRNA). Conventional methods for miRNA detection, including RT-PCR and Northern blot, are limited due to the requirement of cell disruption. Here, we developed a novel synthetic toehold switch, inspired by the toehold switches developed for bacterial systems, to detect endogenous and exogenously expressed miRNAs in mammalian cells, including HEK 293, HeLa, and MDA-MB-231 cells. Transforming growth factor  $\beta$ -induced miR-155 expression in MDA-MB-231 cells could be detected by the synthetic toehold switch. The experimental results showed the dynamic range of current design of toehold switch is about two. Furthermore, we tested multiplex detection of miR-155 and miR-21 in HEK 293 cells by using miR-155 and miR-21 toehold switches. These toehold switches provide a modest level of orthogonality and could be optimized to achieve a better dynamic range. Our experimental results demonstrate the capability of miRNA toehold switch for detecting and visualizing miRNA expression in mammalian cells, which may potentially lead to new therapeutic or diagnostic applications.

**KEYWORDS:** microRNA, miR-155, miR-21, toehold switch, TGF $\beta$ , multiplex detection



Engineering synthetic regulatory genetic circuit in living cells has gained significant interests in the past decade. It provides an effective means to control or regulate cell behaviors for potential applications in human health as well to advance basic research.<sup>1,2</sup> While molecular probes are available for detecting cellular RNA,<sup>3–5</sup> the promise of mammalian synthetic biology is to couple an RNA input to regulate gene expression.<sup>6</sup> Recently, synthetic RNA-based switches that can operate at the transcriptional and posttranscriptional levels have drawn researchers' interests to the application of next-generation therapeutics and diagnostics.<sup>7–10</sup> For example, Chen *et al.* developed a synthetic RNA-based regulatory system for the application of advancing cellular therapies by linking ribozyme-based regulatory devices to growth cytokine targets to control mouse and primary human T-cell proliferation.<sup>11</sup> Chase *et al.* developed an approach to design small molecule responsive microRNAs (miRNAs) for Class 2 ribonuclease III Drosha processing.<sup>12</sup> Li *et al.* developed a toehold-initiated rolling circle amplification approach for individual miRNA visualization *in situ* in single cells.<sup>13–15</sup> They also developed a spinach-based aptamer for low background miRNA detection by coupling transcription amplification with rolling circle amplification (RCA) (AmptSpi assay).<sup>16</sup> In these contexts, RNA-based switchable platforms are needed to report and respond to dynamic cellular changes during cell development and diseases.

miRNAs are small, noncoding RNA molecules with the length of 21–23 nucleotides that play critical roles in different

biological processes including development, proliferation and apoptosis by mediating translational repression through targeting mRNA (mRNA).<sup>17–20</sup> Increasing evidence has shown miRNA plays an important role in human diseases including cancer<sup>21,22</sup> and cardiovascular diseases.<sup>23–25</sup> Aberrant expression of miRNAs that target cancer-associated genes induces cancer initiation, progression, metastasis and drug resistance.<sup>26</sup> For example, in breast cancer, multifunctional miRNA miR-155 and miR-21 have been shown to have distinct expression profiles and play a crucial role in various physiological and pathological processes. Thus, there is a quest to detect and visualize miRNA expression in mammalian cells to effectively study miRNA-regulated signaling pathways for the application of anticancer therapy. Recently, detection of miRNAs in mammalian cell lines using synthetic genetic circuits have been reported by several groups. For example, Haynes *et al.* have developed a synthetic switch that responds to miRNA mimics and becomes activated when the target is presented in U2OS osteosarcoma cells.<sup>27</sup> By engineering a synthetic RNAi sensor, they converted negative regulatory signal into a positive output, which increases the sensitivity and activation in living mammalian cells. Kei *et al.* developed multiple microRNA-responsive synthetic mRNAs for high-resolution identification and separation of living cell types.<sup>28</sup> They found that a set of miRNA-responsive, *in vitro*

Received: December 20, 2018

Published: April 30, 2019

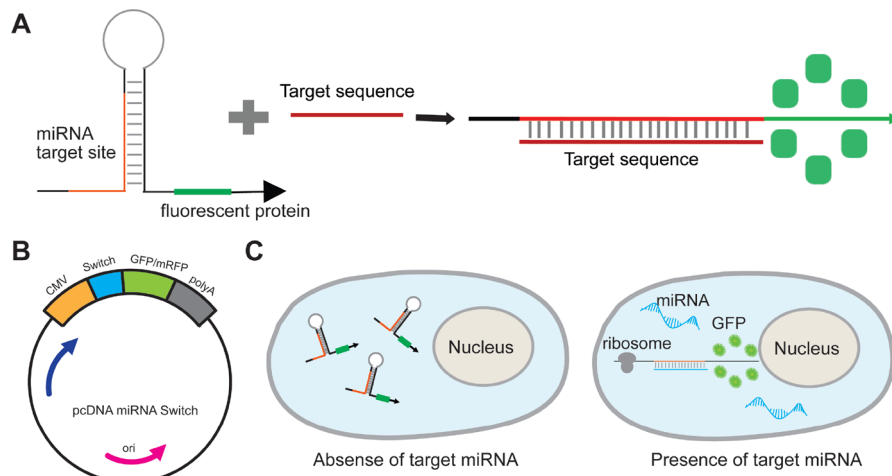


**Figure 1.** Schematic illustration of working principle of synthetic miRNA toehold switch. (A) The toehold structure of synthetic miRNA switch, including miRNA sensing region (red), Kozak sequence and start codon (loop region), and a repressed reporter gene. (B) Construction of miRNA toehold switch plasmid. The miRNA toehold switch sequences were encoded in pcDNA 3.0 plasmid for the detection of the miRNA. (C) Illustration of miRNA detection in mammalian cells using miRNA toehold switch. In the absence of targeted miRNA, the toehold structure is preserved and reporter gene is repressed. In the presence of targeted miRNA, the toehold structure is opened and the reporter gene is expressed.

synthesized mRNAs that can be used to identify and separate specific cell populations based on the differences in miRNA activities. Moreover, the same group developed several miRNA-responsive switches to isolate and separate human pluripotent stem cell (hPSC)-derived cardiomyocytes.<sup>29</sup> Jeremy *et al.* developed an antagonistic/synergistic miRNA repression model to predict multi-input miRNA sensor activity.<sup>30</sup>

Recently, *de novo*-designed riboregulators called toehold switches were developed by Green, Yin, and colleagues that were designed to activate protein translation in response to a trigger RNA.<sup>31</sup> By utilizing toehold-mediated linear–linear interactions<sup>32,33</sup> that avoid any base-pairing with ribosome binding site (RBS) or start codon, the toehold switches could be designed for a trigger RNA of any arbitrary sequence. The toehold switches were applied to both live bacteria as well as freeze-dried cell-free expression systems.<sup>31,34,35</sup> The optimal length of the toehold region was ~30 nt, so it was not immediately clear whether miRNAs could potentially serve as trigger RNAs. Furthermore, the toehold switch design has not been demonstrated in mammalian cells, to the best of our knowledge.

In this study, we developed a novel synthetic toehold switch to detect endogenous and exogenously expressed miRNAs in different mammalian cells, including HEK 293 cells, HeLa cells, and MDA-MB-231 cells. This toehold switch is designed to detect the existence of miRNA in mammalian cells, which enables the visualization of miRNAs at single-cell level. We first designed and evaluated this toehold switch for miRNA detection. We evaluated the performance of this toehold switch by detecting exogenously expressed miRNA-155 in the presence of miRNA-155 mimics/inhibitors in HeLa and MDA-MB-231 cells. We also examined TGF $\beta$ -induced miR-155 expression in MDA-MB-231 cells using this toehold switch. The dynamic range of current design of toehold switches is about two. Finally, multiplex detection of miR-155 and miR-21 in HEK 293 cells were implemented and evaluated by using two synthetic toehold switches (miR-155 and miR-21 toehold switches), thereby testing the orthogonality and programmability of this platform. Our results indicated that these toehold

switches provide a modest level of orthogonality and could be optimized to improve their performance.

## RESULTS AND DISCUSSIONS

**Design of Synthetic miRNA Toehold Switch for miRNA Detection.** The synthetic toehold switches were designed to detect the presence of miRNAs in mammalian cells. We modeled our toehold switch design after the work by Yin's and Collins' groups.<sup>31,35</sup> Previous work has used toehold switches to detect bacterial and viral mRNA; however, this approach has not been demonstrated for detecting mammalian RNA. As shown in Figure 1, miRNA toehold switches include a target sensing region (complementary of the target mature miRNA sequence), the Kozak sequence (GCCACC), start codon (ATG), and repressed gene as a reporter. The target sensing region (labeled in red) was employed at the hairpin stem region, Kozak sequence and start codon were located in the loop of hairpin structure (Figure 1A). The hairpin structure was designed and optimized to achieve high stability and to avoid alternative secondary structures. In the absence of the target miRNAs, the hairpin structure of the miRNA switch is preserved, and GFP is repressed. We suspected that the secondary structure of the hairpin near the Kozak sequence represses translation even though ribosome binds at the 5' cap and the Kozak sequence. In the presence of the target miRNA (transfected in this case), miRNA binding creates dsRNA (which is somehow unwound by the ribosome) to open the stem-loop structure thereby allowing the reporter gene to be expressed (Figure 1A). Here, two miRNA switches, miR-155 and miR-21, were designed and optimized (Figure 1B). A pcDNA-toehold-miR-155 and pcDNA-toehold-miR-21 switch constructs were generated by cloning a DNA fragment encoding miR-155 target site (5'-ACCCC TATCA CGATT AGCAT TAA-3') or miR-21 target site (5'-TAGCT TATCA GACTG ATGTT GA-3'), and GFP or mRFP as a reporter into pcDNA 3.0 vector. The constructs can be transfected to cells and sense endogenous miRNA, exogenously expressed miRNA, or stimulated miRNA expression in living mammalian cells (Figure 1C). The toehold structures for miR-155, miR-21, and control plasmid are shown in Figure S1A–C.

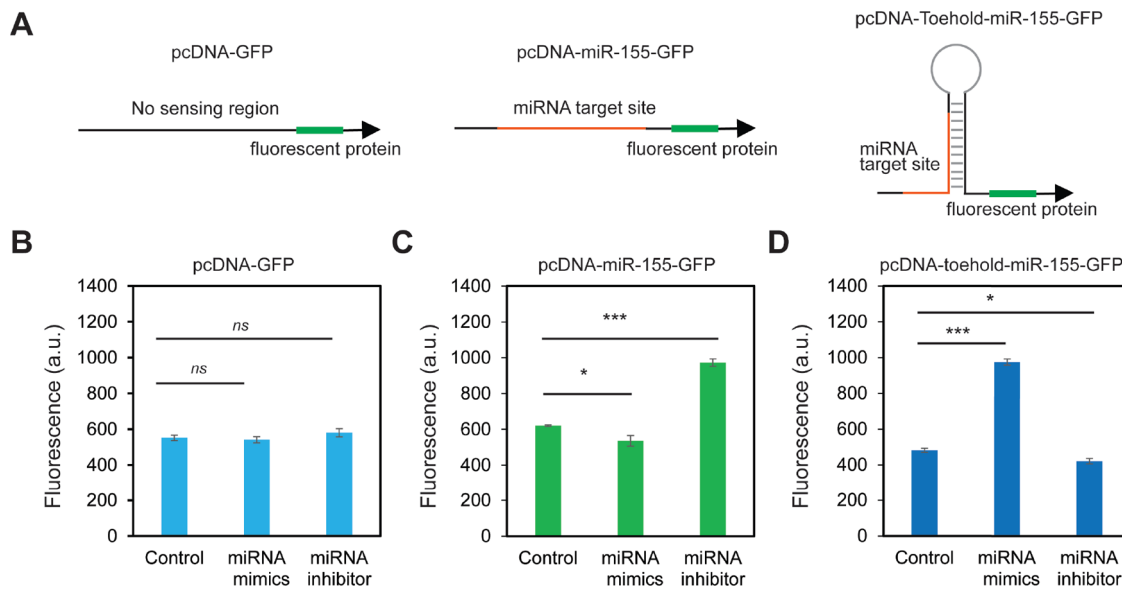


**Figure 2.** Comparison of different switch sensors for detection of exogenously expressed miR-155 in mammalian cells. (A) Three different plasmid designs including a control plasmid without sensing region, a miRNA detecting plasmid without toehold structure, and a miR-155 toehold switch. (B–D) are flow cytometry results of GFP expression in HeLa cells in the presence of miR-155 mimics or miR-155 inhibitor using control plasmid, miR-155 detecting plasmid and miR-155 toehold switch. Experiments were carried out after 48 h transfection. The concentration of DNA plasmid used in this experiment is 500 ng/mL. The concentration of miR-155 mimics, inhibitor and negative control is 25 nM. Data are expressed as mean  $\pm$  s.e.m. ( $n = 3$ ; ns, not significant; \* $p < 0.05$ , \*\* $p < 0.01$ , \*\*\* $p < 0.001$ ; unpaired Student's *t*-test).

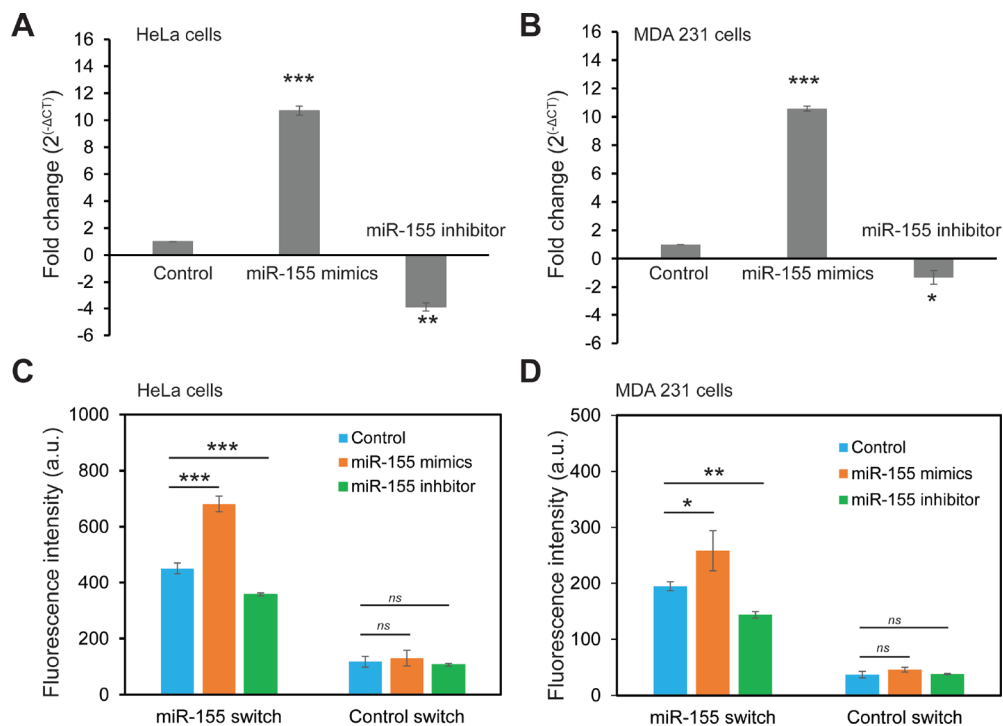


**Figure 3.** Detection of exogenous miR-155 expression in HeLa cells and MDA-MB-231 cells. (A) and (B) are the RT-PCR analysis results of exogenous miR-155 expression in the presence of miR-155 mimics or inhibitor in HeLa cells and MDA 231 cells, respectively. (C) and (D) are flow cytometry results of detection of exogenous miR-155 expression using miR-155 toehold switch and control switch in HeLa cells and MDA-MB-231 cells, respectively. The error bars indicate the mean  $\pm$  s.e.m. ( $n = 3$ ; ns, not significant; \* $p < 0.05$ , \*\* $p < 0.01$ , \*\*\* $p < 0.001$ ; unpaired Student's *t*-test). Note that (C) shows the same condition as Figure 2B,D, but were carried out as a separate set of experiments.

**Characterization of miRNA Toehold Switch.** With the design of the toehold switch, we first characterized the performance of miR-155 toehold switch by comparing it with a nontoe hold miRNA sensor. As shown in Figure 2A, three different plasmids were constructed, a positive control which

includes a fluorescent protein without the miRNA sensing region (pcDNA-GFP), a nontoe hold miRNA sensor that includes a miRNA target site (miR-155 target site) without toehold structure and a fluorescent protein (GFP), and a toehold switch that includes a toehold structure and a

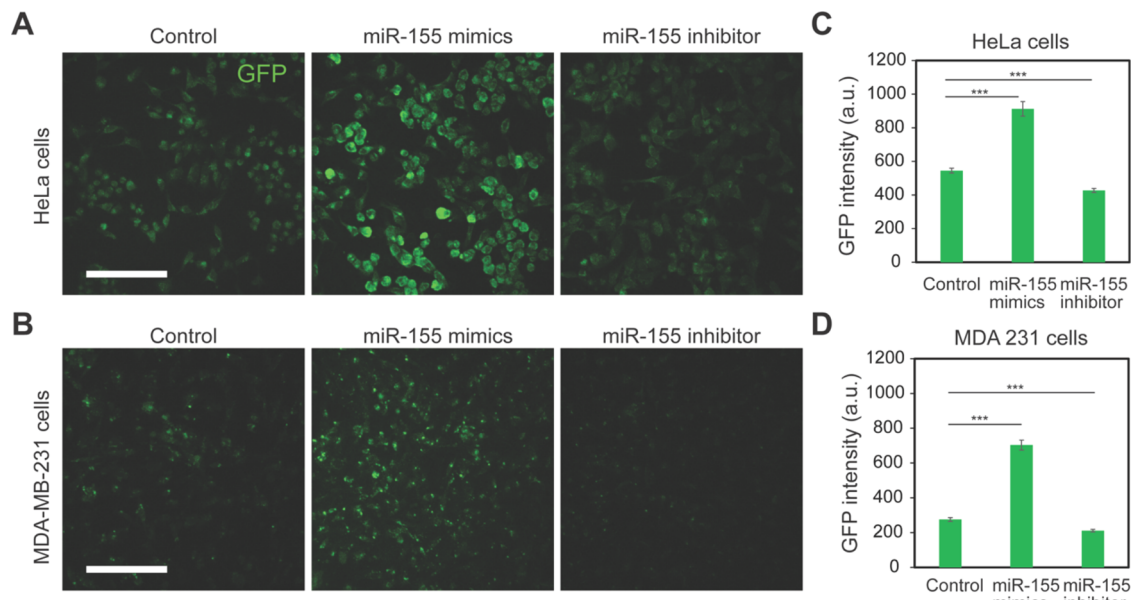


**Figure 4.** GFP expression in HeLa cells and MDA-MB-231 cells in the presence of mimics or inhibitor using miR-155 toehold switch. (A) and (B) are fluorescence images of GFP in the presence of miR-155 mimics or inhibitor in HeLa and MDA-MB-231 cells, respectively. Scale bar: 150  $\mu$ m. (C) and (D) are fluorescence intensity of GFP expression in HeLa cells and MDA-MB-231 cells, respectively. Both HeLa and MDA-MB-231 cells were cotransfected miR-155 switch together with miR-155 mimics, miR-155 inhibitor or negative control (25 nM for each) for 48 h before imaging. The error bars indicate the mean  $\pm$  s.e.m. (\*\*\*) $p < 0.001$ ; unpaired Student's *t*-test). Experiments were repeated twice independently with triplicates.

fluorescent protein. The performance of these three different constructs were evaluated by measuring GFP intensity in HeLa cells. First, HeLa cells were cotransfected with DNA plasmids (pcDNA-GFP, pcDNA-miR-155-GFP, or toehold-miR-155-GFP) with or without miRNA mimics/inhibitors for 48 h. miRNA mimics are chemically synthesized double-stranded RNA molecules that imitate mature miRNA, whereas miRNA inhibitors are single-stranded chemically enhanced oligonucleotides that are designed to inhibit the endogenous miRNA. miRNA mimics have been widely used in synthetic biology for testing genetic circuit and transcriptional gene silencing.<sup>17,20</sup> As shown in Figure 2B, without the sensing region, GFP expression levels in HeLa cells were not significantly different in the presence of miR-155 mimics or inhibitors, as expected. With the sensing region, GFP expression decreased by 13.6% ((GFP intensity in the presence of miR-155 mimics – GFP intensity in control group)/GFP intensity in control group) compared to control in the presence of miR-155 mimics, while GFP expression increased by 56.8% ((GFP intensity in the presence of miR-155 inhibitors – GFP intensity in control group)/GFP intensity in control group) compared to control in the presence of miR-155 inhibitors. With the toehold structure, GFP expression increased by 102.3% in the presence of miRNA-155 mimics while it decreased by 12.4% in the presence of miR-155 inhibitors. These results indicate that both of these miRNA sensors could detect miR-155 in HeLa cells, although the working mechanisms are different. By using toehold miRNA switch, GFP was expressed in the presence of miRNA mimics while it remained repressed in the presence of miRNA inhibitors. Without the toehold structure, GFP expression occurred in the presence of miRNA inhibitor. Thus, our *de novo* designed toehold switch had the capability of detecting miRNAs in mammalian cells.

#### Toehold Switch for Exogenously Expressed miRNA-155 Detection in Mammalian Cells.

To demonstrate the

capability of toehold switch sensor for exogenous detection of miR-155 in mammalian cells, the miR-155 expression levels in HeLa and MDA-MB-231 cells were first analyzed using RT-PCR in the presence of miR-155 mimics or inhibitors, Figure 3A,B. First, in order to validate the miR-155 toehold switch is capable of detecting increased or decreased miRNA levels in mammalian cells, miRNA mimics or inhibitors were delivered into mammalian cells. The endogenous miRNA levels in HeLa cells and MDA-MB-231 cells were analyzed after 48 h delivery. For control group, cells were transfected with equal amount of negative control mimics for comparison. We then performed RT-PCR analysis and confirmed the expression level of miR-155 in HeLa and MDA-MB-231 cells. As shown in Figure 3A,B, miR-155 expression levels were increased about 10-fold in the presence of miR-155 mimics in both HeLa and MDA-MB-231 cells. In the presence of miR-155 inhibitors, the mature miR-155 expression levels were decreased 3.8 and 1.3 fold in HeLa and MDA-MB-231 cells, respectively. The results indicate that mature miR-155 levels can be altered by introducing miRNA mimics and inhibitors. In order to validate the performance of toehold switch, the miR-155 switch sensor was cotransfected with miR-155 mimics (25 nM) or miR-155 inhibitors (25 nM) for 48 h. A control toehold switch was used as negative control. As shown in Figure 3C,D, GFP expression increased in the presence of miRNA-155 mimics in miR-155 toehold switch transfected cells, while GFP expression decreased in the presence of miR-155 inhibitors in both HeLa and MDA-MB-231 cells. For HeLa cells, the miR-155 toehold switch sensor had an increase in fluorescence of about 50% (this was calculated as (GFP intensity in miR-155 mimics group – GFP intensity in control group)/GFP intensity of control group) in the presence of miR-155 mimics compared to control group, indicating the toehold structure was opened due to the delivery of miR-155 mimics, thus the repressed GFP was expressed. In the presence miR-155 inhibitors, the GFP

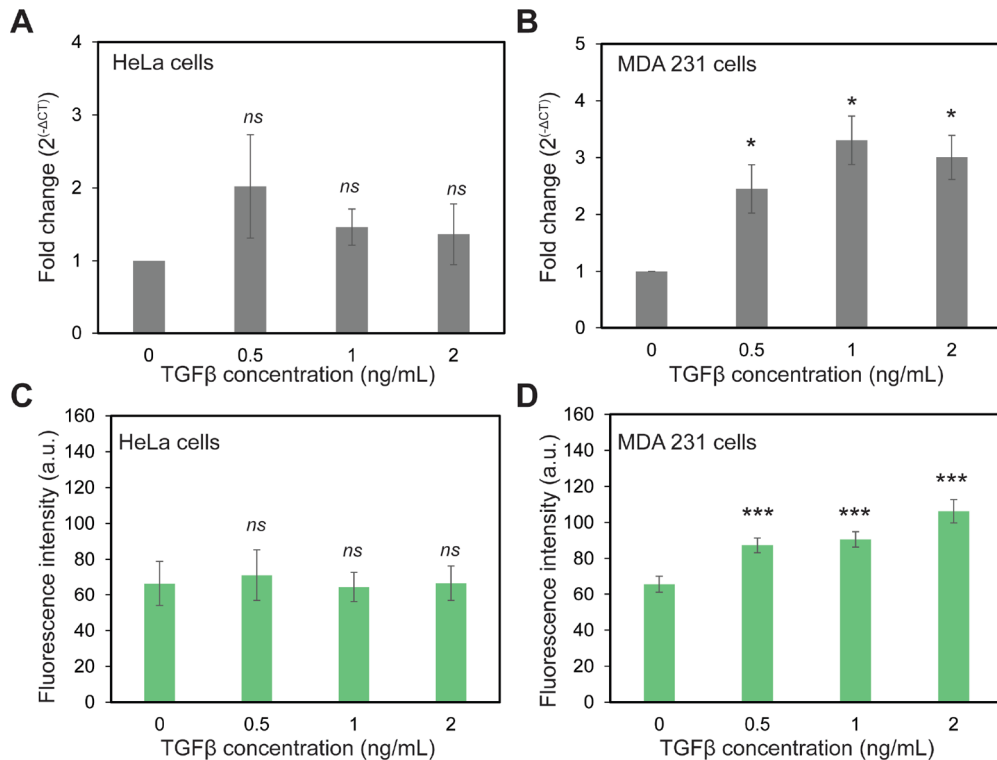


**Figure 5.** Detection of exogenous miR-155 expression in HeLa cells and MDA-MB-231 cells. (A) and (B) are miR-155 expression using RT-PCR in the presence of TGF $\beta$  with the concentrations of 0, 0.5, 1, and 2 ng/mL in HeLa cells and MDA-MB-231 cells, respectively. (C) and (D) are flow cytometry analyses of detection of endogenous miR-155 expression in the presence of TGF $\beta$  with different concentrations using miR-155 toehold switch in HeLa cells and MDA-MB-231 cells, respectively. The error bars indicate the mean  $\pm$  s.e.m. ( $n = 3$ ; ns, not significant; \* $p < 0.05$ , \*\*\* $p < 0.001$ ; unpaired Student's *t*-test).

signal was decreased by about 20% (this was calculated as (GFP intensity in miR-155 inhibitor group – GFP intensity in control group)/GFP intensity of control group) compared to control group. For MDA-MB-231 cells, the GFP expression increased by 33% and decreased by 26% in the presence of miR-155 mimics and miR-155 inhibitors, respectively. These experimental results showed the toehold switch is able to detect exogenous miRNAs in different types of mammalian cells. This toehold switch can detect as low as 1.3 fold change of miRNA levels in mammalian cells, as shown in Figure 3B,D. However, the fold change in fluorescence is quite modest in the presence of miR-155 inhibitors.

Furthermore, in order to visualize miRNA-155 in mammalian cells using miRNA toehold switch, both HeLa cells and MDA-MB-231 cells were cotransfected with miR-155 toehold switch and negative control, miR-155 mimics or miR-155 inhibitors, respectively. Images were acquired after 48 h transfection, as shown in Figure 4A,B. In order to show GFP expression was induced by the presence of miR-155, a control toehold switch was used as a negative control. As shown in Figure S2, there was no green fluorescence detected, indicating the green fluorescence were GFP expression in the presence of miR-155. The fluorescence intensity in each condition was quantified and compared for each cell type (Figure 4C,D). For both cell types, GFP expressions increased in the presence of miR-155 mimics, while the GFP expression decreased in the presence of miR-155 inhibitors. These results are consistent with the flow cytometry results shown in Figure 3C,D, and support the use of miR-155 toehold switch to visualize miRNAs expression and quantify the relative expression levels in different types of mammalian cells.

#### Toehold Switch for Endogenous miRNA-155 Detection in Mammalian Cells.

We further investigated the possibility of using the toehold switch for detecting stimulated endogenous miR-155 expression in HeLa and MDA-MB-231 cells. First, in order to induce miR-155 expression, we performed TGF $\beta$  administration to both HeLa and MDA-MB-231 cells. TGF $\beta$  is a cytokine that is known to induce epithelial-to-mesenchymal transition (EMT).<sup>36</sup> It has been shown that TGF $\beta$  induces miR-155 expression in invasive breast cancer cells and promotes cell invasion and migration.<sup>37–39</sup> Both HeLa and MDA-MB-231 cells were treated with different concentrations of TGF $\beta$  for 48 h. Then miR-155 expression levels were quantified and analyzed using RT-PCR. As shown in Figure 5A, miR-155 expression was not significantly different compared to the control group in TGF $\beta$ -treated HeLa cells. In contrast, TGF $\beta$ -treated MDA-MB-231 had markedly increased miR-155 expression levels compared to the control group. The miR-155 expression level increased by 2.5, 3.3, and 3 folds with TGF $\beta$  concentrations of 0.5, 1, and 2 ng/mL, respectively. Further increase of TGF $\beta$  concentration did not further upregulate miR-155 expression (Figure S3). Next, miR-155 toehold switch was used to detect the endogenous miR-155 induced by TGF $\beta$  in both HeLa and MDA-MB-231 cells. The cells were transfected with miR-155 toehold switch and treated with TGF $\beta$  at three different concentrations (0.5, 1, and 2 ng/mL). As shown in Figure 5C, the GFP expressions, as measured by flow cytometry analysis, in HeLa cells were not significantly different with the treatments of TGF $\beta$ , indicating the miR-155 expression levels were the same as the control group without TGF $\beta$  treatment, consistent with the RT-PCR results. In contrast, the GFP

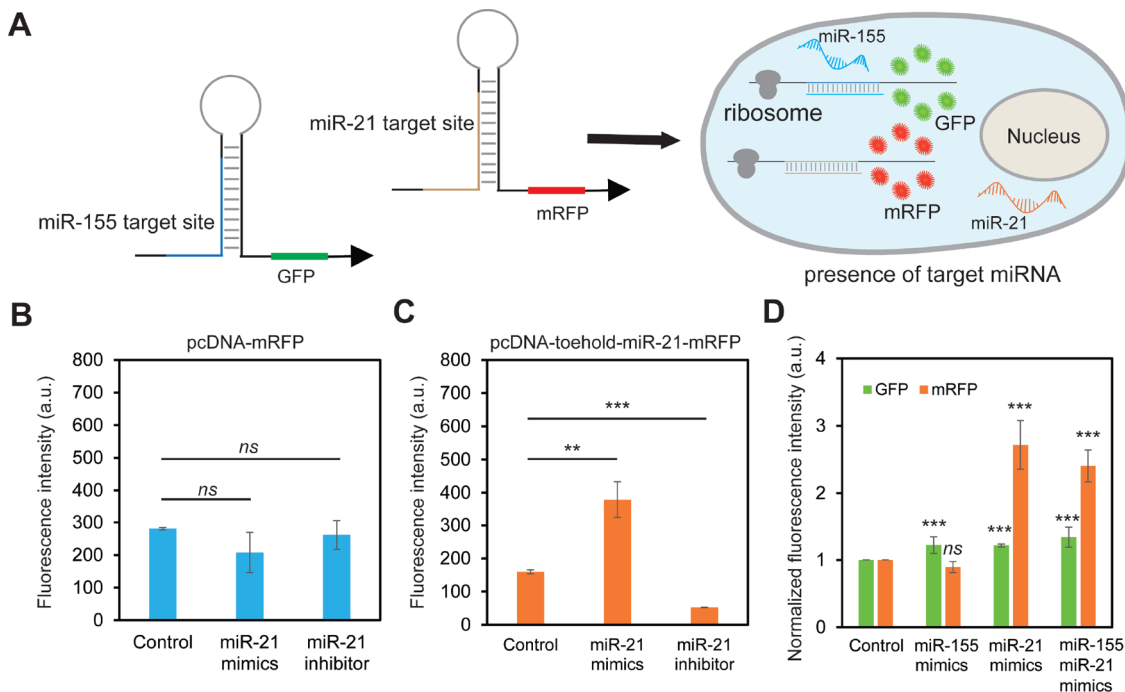


**Figure 6.** Multiplex detection of miRNAs in mammalian cells using synthetic miR-155 switch and miR-21 switch sensors. (A) Schematic illustration of multiplex miRNA detection using synthetic miRNA switch sensor. miR-21 switch sensor was designed according to the same design principle of miR-155 switch sensor. Instead of using GFP as a repressing gene, mRFP was used in miR-21 switch sensor. (B) Flow cytometry results of mRFP expression in the presence of miR-21 mimics or miR-21 inhibitor in HEK 293 cells using pcDNA-mRFP control plasmid. (C) Flow cytometry results of mRFP expression in the presence of miR-21 mimics or miR-21 inhibitor in HEK 293 cells using miR-21 switch sensor. (D) Flow cytometry results of multiplex detection of miR-155 and miR-21 expression in HEK 293 cells. The fluorescence intensity of GFP and mRFP in control groups were normalized to 1 for comparison. GFP expression indicates exogenous miR-155 expression levels and mRFP expression indicates exogenous miR-21 expression levels. Data are expressed as mean  $\pm$  s.e.m. ( $n = 3$ ; ns, not significant; \*\* $p < 0.01$ , \*\*\* $p < 0.001$ ; unpaired Student's *t*-test).

expression in MDA-MB-231 cells increased with TGF $\beta$  treatments at all three concentrations (Figure 5D). The cumulative probability of GFP intensity in HeLa and MDA-MB-231 cells confirmed the effects of TGF $\beta$  on the regulation of miR-155 expression (Figure S4). These experimental results indicate that the toehold switch can detect endogenous miRNA expression induced by growth factor stimulation. Since different molecules have different effects on the miRNA expression (upregulation or downregulation), one potential application of this toehold switch is to identify or separate different types of cells, similar to using synthetic miRNA switches to isolate human pluripotent stem cell (hPSC)-derived cardiomyocytes and purify various cell types that Miki *et al.* has demonstrated.<sup>29</sup> The challenge of isolation and purification of various cell types using our toehold switch may be the low expression of miRNA in mammalian cells. It will be challenging to isolate cell types that have similar expressions of miRNA. This can be improved by optimizing the sensitivity of toehold switch, which may be achieved by changing hairpin structures, changing the length of hairpin stem and loop to optimize the ON/OFF ratio.

**Multiplex Detection of miRNAs in Mammalian Cells Using Synthetic Toehold Switches.** A feature of our *de novo* synthetic toehold switches is the orthogonality between different miRNA switches. To test this, we implemented multiplex detection of miRNAs by using miR-155 toehold switch and miR-21 toehold switch. As shown in Figure 6A, miR-21 toehold switch together with miR-155 toehold switch can be cotransfected into mammalian cells for detecting of

miR-155 and miR-21 in different cell lines. A miR-21 toehold switch was designed according to the same design principle as the miR-155 toehold switch. The toehold structure was optimized to make sure the start codon was in the stem region and mRFP expression was repressed. The performance of miR-21 toehold switch was tested in human embryonic kidney 293 (HEK 293) cells. We used miR-21 mimics and inhibitors to increase or decrease the miR-21 expressions in HEK 293 cells, similar to the strategy we employed for miR-155. As a control construct without a toehold sensing region, mRFP expression in HEK 293 cells did not have significant difference with miR-21 mimics or miR-21 inhibitors. Meanwhile, mRFP expression increased by ~1.4 fold ((mRFP expression in the presence of miR-21 mimics – mRFP expression in control group)/mRFP expression in control group) in the presence of miR-21 mimics and decreased by ~0.7 fold in the presence of miR-21 inhibitors using miR-21 toehold switch (Figure 6C). These results showed that miR-21 toehold switch sensor can detect the presence of miR-21 in HEK 293 cells. Four groups of experiments were performed to test the effectiveness of multiplex detection of miRNAs in HEK 293 cells transfected with miR-155 and miR-21 toehold switches. The first group of HEK 293 cells were only transfected with miRNA mimics negative control; the second and third groups were transfected with miR-155 mimics and miR-21 mimics, respectively. The last group were cotransfected with both miR-155 and miR-21 mimics. In the presence of miR-155 mimics, the GFP intensity increased by 0.22 fold compared to the control group, while the mRFP intensity did

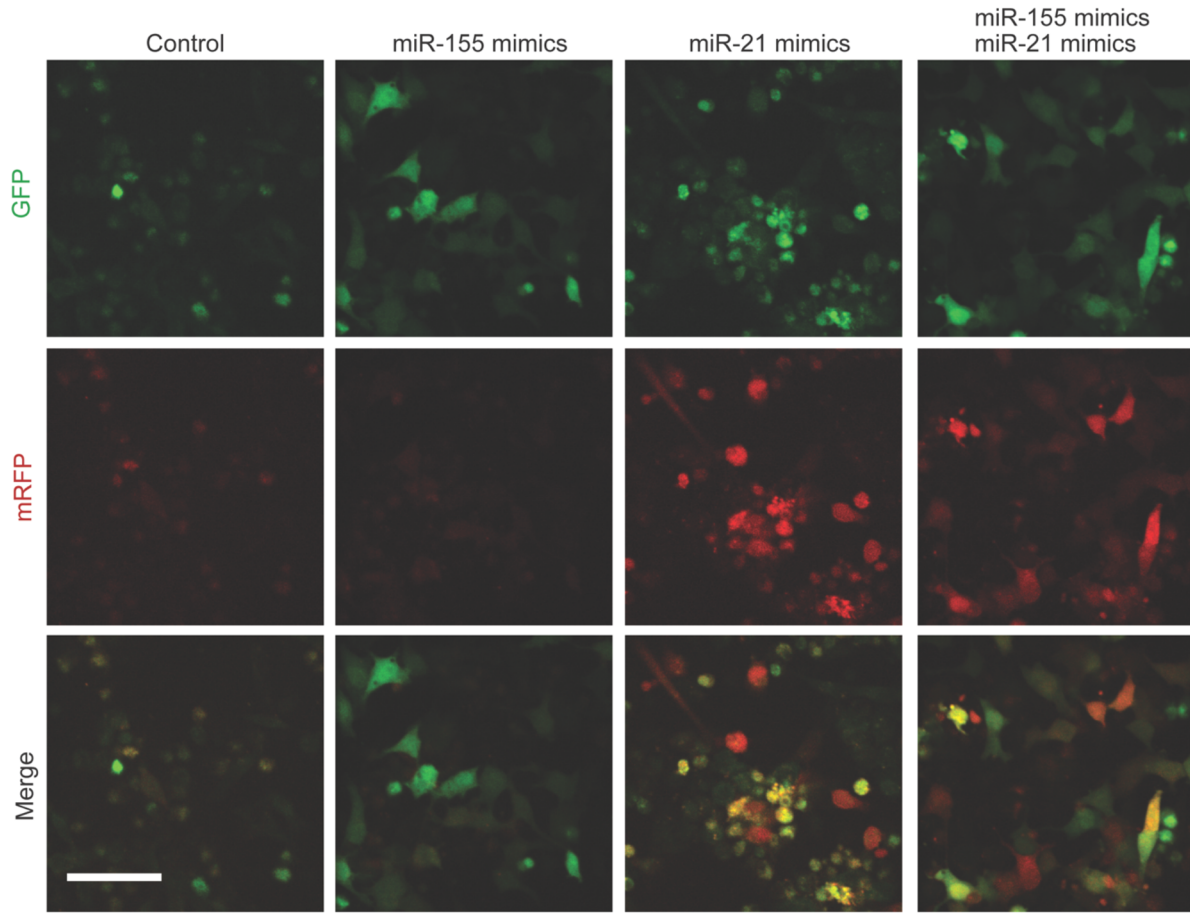


**Figure 7.** Multiplex detection of exogenous miR-155 and miR-21 expression in HEK 293 cells. (A) Fluorescence microscopy images of GFP and mRFP expression in the presence of miR-155 mimics, miR-21 mimics or both miR-155 and miR-21 mimics. Green fluorescence indicates GFP expression and red fluorescence indicates mRFP expression. HEK 293 cells were transfected with equal amount of DNA plasmid (500 ng/mL) and miRNA mimics (25 nM) for 48 h before imaging. Scale bar: 50  $\mu$ m. Experiments were repeated three times with triplicates.

not show significant changes compared to the control group, consistent with the interpretation that the miR-155 switch, but not the miR-21 switch, was turned on due to the presence of miR-155 mimics (Figure 6D). In the presence of miR-21 mimics, the GFP intensity increased by 0.21 fold while the mRFP intensity increased by 1.7 fold compared to the control groups. This indicates that the miR-21 toehold switch was turned on in the presence of miR-21 mimics. However, to our surprise, there was GFP leakage in the miR-155 toehold switch caused by miR-21 mimics. When miR-21 and miR-155 mimics were both transfected in HEK 293 cells expressing miR-21 and miR-155 toehold switches, the GFP and mRFP intensity increased by 0.3 folds and 1.4 folds compared to control, respectively. The increase of mRFP intensity was due to the presence of miR-21 mimics while we believe the increase of GFP intensity was partially due to the presence of miR-21 mimics. Consistent with the flow cytometry analysis, fluorescence images of GFP and mRFP expression in HEK 293 increased with miR-155 and miR-21 mimics, respectively (Figure 7). However, we also observed GFP leakage when miR-21 was transfected. With miR-155 and miR-21 mimics, both GFP and mRFP intensity showed significant increases compared to control group. These results indicate that the miR-155 switch is not as specific to detect the miR-155 expressions since the miR-21 mimics could also increase GFP expression. The GFP leakage in the miR-155 switch could

potentially be mitigated by adjusting the number of nucleotides in the stem region. However, both the miR-155 switch and the miR-21 switch showed good performance in detecting single miRNAs.

## CONCLUSION

In this work, we developed a novel synthetic toehold switch for miRNA detection and visualization in different types of mammalian cells. We first characterized the performance of this toehold switch by comparing GFP intensity in three different constructs. The miR-155 toehold switch has a better dynamic range than compared to previously reported miRNA sensors. Our miRNA toehold switch was utilized to sense exogenous and endogenous miRNAs. We demonstrated that this toehold switch is capable of detecting intracellular level of miRNAs. Although the toehold switch functions as designed for miR-155, multiplex detection of different miRNAs revealed that the specificity of miR-155 toehold switch requires further optimization. The leakage of this toehold switch may be caused by nonspecific binding, which could be remedied by adjusting the stem and loop sizes. Nevertheless, this miRNA toehold switch-based platform presents two important advances in mammalian synthetic biology. First, this platform has the potential of identifying different cell types based on miRNA levels. Second, this platform can be extended to sense and program mammalian cells based on the intracellular levels of

miRNAs. The ability to couple sensing of endogenous changes in miRNA concentrations to regulate protein translation could provide a powerful approach to rewire mammalian cell functions that may lead to novel therapeutic strategies.

## MATERIALS AND METHODS

**Plasmid Construction.** All the switch plasmids were constructed using standard cloning techniques. Competent *E. coli* strain DH5 $\alpha$  was used for cloning purposes and was grown in LB Broth Miller medium with appropriate antibiotics (Ampicillin, 100  $\mu$ g/mL, Kanamycin, 50  $\mu$ g/mL). All the DNA fragments and primer sequences were synthesized by IDT (Integrated DNA Technologies). All enzymes were purchased from New England Biolabs (NEB). Digestion products and PCR products were purified using Wizard SV Gel and PCR Clean-Up System (Promega Corporation). All ligation were performed using T4 DNA ligase (NEB) with adjusted incubation time and temperature. The ligation products were then transformed into chemically competent *E. coli* DH5 $\alpha$  and plated on LB Agar plates with appropriate antibiotics. All the plasmid DNA was prepared from *E. coli* using Wizard Plus SV Minipreps DNA purification system (Promega, Madison, WI). After plasmid purification, the DNA amounts were quantified using Nanodrop (ND-2000). All the constructed plasmids were sequenced and identified using appropriate primers by Sanger sequencing at DNA Sequencing Core, University of Michigan. All the toehold structure sequences and sequencing results are listed in [Supplementary Methods](#).

The pcDNA-toehold-miR-155-switch plasmid was created by cloning a DNA fragment encoding miR-155 target sequence (completely complementary to the mature miR-155 at the 5' UTR), and reporter gene green fluorescence protein (GFP) between Xhol and BamHI restriction sites in pcDNA 3.0. The coding region of miR-155-switch was PCR amplified using the primers Xhol forward primer (5'-TAAGC TCTCG AGAAA ACCCC TATCA CGATT-3') and BamHI reverse primer (5'-CGTCA GGATCC TTAT TAAAC TGATG CAGCG-3'). The resulting DNA fragment was digested with XhoI and BamHI and cloned downstream of the CMV promoter between the XhoI and BamHI cloning sites to result in pcDNA-toehold-miR-155-switch plasmid. This plasmid serves as a sensor for the detection of presence of miR-155 in mammalian cells. The pcDNA-miR-155-GFP plasmid was constructed using site-directed mutagenesis method. The toehold sequence (5'-AATTAA ATGCT AAAAA CCTGG CGGCA GCGCA AAAG-3') was deleted from pcDNA-toehold-miR-155 plasmid using a pair of standard primers (Forward primer: 5'-ATTTT CCATC AAGAA CAGGC CACCT CGCCA CCATG GTGAG CA-3', reverse primer: 5'-TAATG CTAAT CGTGA TAGGG GTTTT GGTAG CGCTA GCGGA TCTG-3').

The pcDNA-control-switch plasmid was created by cloning the DNA fragment encoding control switch sequences and GFP protein between Xhol and BamHI restriction sites in pcDNA 3.0. The control switch sequences were designed to have toehold structure without miRNA sensing region. The coding region of control switch was amplified through PCR using XhoI forward primer (5'-TAAGCT CTCGAG GGGTA TGTAAT TTGAT TTGGC TTCTGT-3') and BamHI reverse primer (5'-CGTCA GGATC CTTAT TAAAC TGATG CAGCG-3'). The resulting DNA fragment was digested with XhoI and BamHI and cloned downstream of the CMV promoter between the XhoI and BamHI cloning sites to result

in pcDNA-control-switch plasmid. This plasmid serves as a negative control for the background GFP protein detection.

The pcDNA-toehold-miR-21-monomer red fluorescent protein (mRFP) switch was constructed using site-directed mutagenesis method. Toehold-miR-21 sequence including the stem region and loop region was designed and synthesized by IDT. The miR-21 detection sequence is the complementary strand of mature miR-21 sequence. The miR-21 detection sequence was encoded in the stem region (5'-TCAAC ATCAG TCTGA TAAGC TA-3'). The custom-designed miR-21 toehold sequence was inserted into pcDNA 3.0-mRFP plasmid (Addgene) using Q5 site-directed mutagenesis kit with a pair of back-to-back orientated primers. (Forward primer: 5'-AGGCC ACCAT GGAAA ATAGC TTATC AGAAA TATAT AAAAA AACAC TGGCG GCCGC TCGA-3', Reverse primer: 5'- TTCTT GATGG AAAAT AGCTT ATCAG ACTGA TGTG AAAAT TTGAT GGATA TCTGC AGAAT TCCAG CACAC TGG-3'). The PCR product was analyzed using agarose gel electrophoresis before KLD enzyme mix reaction. This plasmid was used to detect the presence of miR-21 in mammalian cells.

**Design of Synthetic miRNA Switch Sensor.** The miRNA switch sensor was designed to detect the presence of miRNAs in mammalian cells. The synthetic miRNA switch includes a target sensing region, Kozak sequence (GCCACC), start codon (ATG), and a repressed gene as a reporter. The design principle is that the target sensing region will be employed at the hairpin stem region, Kozak sequence and start codon will be employed in the loop of hairpin structure. For the miR-155 switch, the miR-155 sensing region sequence is AAAAC CCCTA TCACG ATTAG CATTA ATTTT CCATC AAGAA CAGGC CACCA TGGAA AATTA ATGCT AAAAA CCTG GCGGC AGCGC AAAAG (5'-3'). For miRNA-21 switch, the toehold structure sequence is AAATT TTCAA CATCA GTCTG ATAAG CTATT TTCCA TCAAG AACAG GCCAC CATGG AAAAT AGCTT ATCAG AAATA TATAA AAAA (5'-3'). The free energy change ( $\Delta G$ ) for miRNA-155 and miRNA-21 switch were calculated as -18.7 and -18.22 kcal/mol using mFold software, respectively.

**Cell Culture.** All the cell lines were cultured at 37 °C and 5% CO<sub>2</sub> in tissue culture dishes in a humidified incubator. Media were changed every 2 days. Human embryonic kidney (HEK) 293 (ATCC) and HeLa cells (ATCC) were cultured in Dulbecco's Modified Eagle Media (DMEM), high glucose (Thermo Fisher Scientific), supplemented with 10% FBS and 1% Penicillin/Streptomycin solution. MDA-MB-231 cells were acquired from ATCC and cultured in RPMI-1640 media with 25 mM HEPES and L-Glutamine (Sigma-Aldrich), supplemented with 10% FBS, 1% Penicillin/Streptomycin solution, and 5  $\mu$ g/mL Gibco Gentamycin (Thermo Fisher Scientific). All cells were trypsinized using 0.25% Trypsin-EDTA.

**Transfections.** All the DNA plasmids transfections were performed using Lipofectamine 2000 Transfection Reagent (Life Technologies). All transfections were performed in 6-well plates (Thermo Scientific). One day before transfection, cells were seeded at a density of  $3 \times 10^5$  per well with 1.5 mL medium. Transfections were performed when the cells reach 70–80% confluence. The DNA plasmids were diluted in 150  $\mu$ L Opti-MEM I Reduced Serum Media (Thermo Fisher Scientific) per well. The DNA concentration used for transfection is 500 ng/mL. Lipofectamine 2000 was used in amounts of 6  $\mu$ L per sample and was mixed with 150  $\mu$ L Opti-

MEM. After 5 min incubation at room temperature, the diluted Lipofectamine was mixed with the diluted DNA samples and incubated at room temperature for 20 min before adding to the cells.

For all miRNA mimics alone, transfections were performed using Lipofectamine RNAiMax transfection reagent according to manufacturer's protocol. All miRNA mimics and inhibitors were purchased from ThermoFisher Scientific. The miR-155 mimics and miR-21 mimics sequences were 5'-UUAAU GCUAA UUGUG AUAG GGGU-3' (Assay ID. MC28440; Cat no. 4464066) and 5'-UAGCU UAUC AGACU GAUG UUGA-3' (Assay ID. MC10206; Cat no. 4464066), respectively. For control group, cells were transfected with equal amount of negative control mimics for comparison. The sequences for miR-155 inhibitor (Assay ID. MC28440; Cat no. 4464084), miR-21 inhibitor (Assay ID. MC10206; Cat no. 4464084), and negative control mimics (Cat no. 4464058) were not disclosed from the product information. The concentration of miR-155 mimics, inhibitor and negative control is 25 nM. For plasmid DNA and miRNA mimics cotransfection, Lipofectamine 2000 transfection reagent were used. The concentration of DNA plasmid used in this experiment is 500 ng/mL. Briefly, plasmid DNA and miRNA mimics were diluted in Opti-MEM and mixed with Lipfectamine 2000 to form DNA-miRNA mimics-Lipofectamine 2000 complexes, following 20 min incubation before adding the complexes into each well containing cells and medium. After 48 h transfection, cells were ready to be analyzed.

**Reverse Transcription and RT-PCR.** For miRNA quantification, the TaqMan MicroRNA RT Kit and TaqMan MiRNA Assays (Life Technologies) were used to generate cDNA and to quantitatively detect mature miRNAs, respectively. In addition, the TaqMan MicroRNA Cells-to-CT Kit (Life Technologies) was used to quantify the levels of mature miRNAs in cells. Briefly, cells were washed with cold 1× phosphate-buffered saline (PBS) for three times and aspirated. Lysis solution (50 μL per well) were added and mixed. Cells were then lysed during this incubation and RNA was released into the lysis solution which contained reagents to inactivate endogenous RNases. Next, stop solution (5 μL per well) was mixed to inactivate the lysis reagents to avoid inhibition of reverse transcription and PCR. For the detection of miRNA, total RNA including miRNA was reverse transcribed using a Taqman miRNA-specific stem-looped primer. Finally, the RT product was amplified by real-time PCR using TaqMan Universal PCR Master Mix and TaqMan MicroRNA Assay according to manufacturer's protocol. A total of 20 μL volume RT-PCR reaction solution was prepared using Taqman Master Mix, 5 μM primer, 25 μM Taqman probe, RT product and nuclease-free water. The quantitative PCR was performed on a BioRad Real Time PCR system, and data were collected and analyzed. All samples were prepared and tested in triplicate. Experiments were performed at least three times independently. To calculate relative concentration, C<sub>T</sub> values for all samples were obtained. ΔC<sub>T</sub> is a normalized, relative gene expression level. This is accomplished by normalization of miR-155 expression with treatment of mimics or inhibitors to the expression with miR-155 without treatment. A normalized expression for each sample was obtained by subtracting the C<sub>T</sub> value of miR-155 by the same sample's C<sub>T</sub> value and designated as ΔC<sub>T</sub>. This value was then transformed by performing log(2<sup>-(ΔCT)</sup>) for comparing fold change.

**Flow Cytometry.** Cells were prepared in 6-well plates at a density of 3 × 10<sup>5</sup> cells per well and transfected the following day. After 48 h transfection, cells were harvested using 0.25% EDTA-Trypsin and resuspended in 500 μL cold 1% BSA/PBS solution. Cells were then transferred to a microcentrifuge tube and kept on ice. All the cells were analyzed using a Guava EasyCyte Flow Cytometer (Merck Millipore). A total of 10 000 cells were analyzed for each sample. For flow cytometric analysis to detect GFP, a 488 nm excitation laser and Green-B 525/30 nm filter were used. To detect mRFP, we used a 488 nm excitation laser and Red-B 695/50 nm filter were used. For each experiment, nonfluorescent cells (non-treated) were used to adjust the setting to minimize the auto fluorescence signal. The background signal was then subtracted by setting the threshold gate above the signal from nontreated cells. Data were collected and analyzed using Incyte Software (Millipore, USA), and mean fluorescence intensities were presented for comparison.

**Imaging.** Cells were seeded in 35 mm glass-bottom well plates at a density of 1 × 10<sup>5</sup> cells per well. Cells were transfected the next day for 48 h. Before imaging, the culture medium was removed and washed 3 times using 1× PBS. Fluorescence images of transfected cells were acquired with appropriate excitation light and filter cubes using an Olympus DSU-IX81 Spinning Disc Confocal Microscope equipped with an EMCCD camera (iXon X3, Andor) and CSU-X1 (Yokogawa). All images were acquired under the same exposure time of 500 ms for comparison.

**Data Analysis.** Data are presented as mean ± s.e.m. Experiments were conducted in triplicate, and repeated at least three independent times. Student's *t* tests were performed to analyze statistical significance between experimental groups. Statistically significant *p* values were assigned as follows: \**p* < 0.05, \*\**p* < 0.01, or \*\*\**p* < 0.001.

## ASSOCIATED CONTENT

### Supporting Information

The Supporting Information is available free of charge on the ACS Publications website at DOI: [10.1021/acssynbio.8b00530](https://doi.org/10.1021/acssynbio.8b00530).

Figures S1–S4, Tables S1–S2 ([PDF](#))

## AUTHOR INFORMATION

### Corresponding Author

\*Tel: 734-764-7719. E-mail: [allenliu@umich.edu](mailto:allenliu@umich.edu).

### ORCID

Allen P. Liu: [0000-0002-0309-7018](https://orcid.org/0000-0002-0309-7018)

### Present Addresses

<sup>†</sup>Tagliatela College of Engineering, University of New Haven, West Haven, Connecticut 06516, United States.

<sup>#</sup>Department of Biomedical Engineering, Boston University, Boston, Massachusetts 02215, United States.

### Notes

The authors declare no competing financial interest.

## ACKNOWLEDGMENTS

We thank Alex Green (Arizona State University) for sharing bacteria toehold switch design that motivated the present work. The authors would like to thank Maxwell DeNies for his help with plasmid cloning. Funding for the work was provided in part by the gift from Kendall and Susan Warren.

## ■ REFERENCES

- (1) Greber, D., and Fussenegger, M. (2007) Mammalian synthetic biology: engineering of sophisticated gene networks. *J. Biotechnol.* 130 (4), 329–345.
- (2) Xie, M., Haellman, V., and Fussenegger, M. (2016) Synthetic biology—application-oriented cell engineering. *Curr. Opin. Biotechnol.* 40, 139–148.
- (3) Wang, S., Majumder, S., Emery, N. J., and Liu, A. P. (2018) Simultaneous monitoring of transcription and translation in mammalian cell-free expression in bulk and in cell-sized droplets. *Synth. Biol. (Oxford, U. K.)* 3 (1), ysy005.
- (4) Pothoulakis, G., Ceroni, F., Reeve, B., and Ellis, T. (2014) The spinach RNA aptamer as a characterization tool for synthetic biology. *ACS Synth. Biol.* 3 (3), 182–7.
- (5) Chatterjee, G., Chen, Y.-J., and Seelig, G. (2018) Nucleic acid strand displacement with synthetic mRNA inputs in mammalian cells. *ACS Synth. Biol.* 7 (12), 2737–2741.
- (6) Deans, T. L., Cantor, C. R., and Collins, J. J. (2007) A tunable genetic switch based on RNAi and repressor proteins for regulating gene expression in mammalian cells. *Cell* 130 (2), 363–72.
- (7) Messina, A., Langlet, F., Chachlaki, K., Roa, J., Rasika, S., Jouy, N., Gallet, S., Gaytan, F., Parkash, J., and Tena-Sempere, M. (2016) A microRNA switch regulates the rise in hypothalamic GnRH production before puberty. *Nat. Neurosci.* 19 (6), 835.
- (8) Wroblewska, L., Kitada, T., Endo, K., Siciliano, V., Stillo, B., Saito, H., and Weiss, R. (2015) Mammalian synthetic circuits with RNA binding proteins for RNA-only delivery. *Nat. Biotechnol.* 33 (8), 839.
- (9) Endo, K., Hayashi, K., Inoue, T., and Saito, H. (2013) A versatile cis-acting inverter module for synthetic translational switches. *Nat. Commun.* 4, 2393.
- (10) Chang, A. L., Wolf, J. J., and Smolke, C. D. (2012) Synthetic RNA switches as a tool for temporal and spatial control over gene expression. *Curr. Opin. Biotechnol.* 23 (5), 679–688.
- (11) Chen, Y. Y., Jensen, M. C., and Smolke, C. D. (2010) Genetic control of mammalian T-cell proliferation with synthetic RNA regulatory systems. *Proc. Natl. Acad. Sci. U. S. A.* 107 (19), 8531–8536.
- (12) Beisel, C. L., Chen, Y. Y., Culler, S. J., Hoff, K. G., and Smolke, C. D. (2011) Design of small molecule-responsive microRNAs based on structural requirements for Drosha processing. *Nucleic Acids Res.* 39 (7), 2981–2994.
- (13) Deng, R., Zhang, K., and Li, J. (2017) Isothermal amplification for microRNA detection: from the test tube to the cell. *Acc. Chem. Res.* 50 (4), 1059–1068.
- (14) Deng, R., Zhang, K., Sun, Y., Ren, X., and Li, J. (2017) Highly specific imaging of mRNA in single cells by target RNA-initiated rolling circle amplification. *Chem. Sci.* 8 (5), 3668–3675.
- (15) Deng, R., Tang, L., Tian, Q., Wang, Y., Lin, L., and Li, J. (2014) Toehold-initiated rolling circle amplification for visualizing individual microRNAs *in situ* in single cells. *Angew. Chem.* 126 (9), 2421–2425.
- (16) Tang, X., Deng, R., Sun, Y., Ren, X., Zhou, M., and Li, J. (2018) Amplified Tandem Spinach-Based Aptamer Transcription Enables Low Background miRNA Detection. *Anal. Chem.* 90 (16), 10001–10008.
- (17) Jansson, M. D., and Lund, A. H. (2012) MicroRNA and cancer. *Mol. Oncol.* 6 (6), 590–610.
- (18) Hayes, J., Peruzzi, P. P., and Lawler, S. (2014) MicroRNAs in cancer: biomarkers, functions and therapy. *Trends Mol. Med.* 20 (8), 460–9.
- (19) Lin, S., and Gregory, R. I. (2015) MicroRNA biogenesis pathways in cancer. *Nat. Rev. Cancer* 15 (6), 321–33.
- (20) Suzuki, H. I., Katsura, A., Matsuyama, H., and Miyazono, K. (2015) MicroRNA regulons in tumor microenvironment. *Oncogene* 34 (24), 3085–94.
- (21) Bachour, T., and Bennett, K. (2011) The Role of MicroRNAs in Breast Cancer. *J. Assoc. Genet. Technol.* 37 (1), 21–8.
- (22) Sassen, S., Miska, E. A., and Caldas, C. (2008) MicroRNA: implications for cancer. *Virchows Arch.* 452 (1), 1–10.
- (23) Thum, T., Catalucci, D., and Bauersachs, J. (2008) MicroRNAs: novel regulators in cardiac development and disease. *Cardiovasc. Res.* 79 (4), 562–70.
- (24) Urbich, C., Kuehbacher, A., and Dimmeler, S. (2008) Role of microRNAs in vascular diseases, inflammation, and angiogenesis. *Cardiovasc. Res.* 79 (4), 581–8.
- (25) Ono, K., Kuwabara, Y., and Han, J. (2011) MicroRNAs and cardiovascular diseases. *FEBS J.* 278 (10), 1619–33.
- (26) Nana-Sinkam, S. P., and Croce, C. M. (2011) MicroRNAs as therapeutic targets in cancer. *Transl. Res.* 157 (4), 216–225.
- (27) Haynes, K. A., Ceroni, F., Flicker, D., Younger, A., and Silver, P. A. (2012) A sensitive switch for visualizing natural gene silencing in single cells. *ACS Synth. Biol.* 1 (3), 99–106.
- (28) Endo, K., Hayashi, K., and Saito, H. (2016) High-resolution identification and separation of living cell types by multiple microRNA-responsive synthetic mRNAs. *Sci. Rep.* 6, 21991.
- (29) Miki, K., Endo, K., Takahashi, S., Funakoshi, S., Takei, I., Katayama, S., Toyoda, T., Kotaka, M., Takaki, T., and Umeda, M. (2015) Efficient detection and purification of cell populations using synthetic microRNA switches. *Cell Stem Cell* 16 (6), 699–711.
- (30) Gam, J. J., Babb, J., and Weiss, R. (2018) A mixed antagonistic/synergistic miRNA repression model enables accurate predictions of multi-input miRNA sensor activity. *Nat. Commun.* 9 (1), 2430.
- (31) Green, A. A., Silver, P. A., Collins, J. J., and Yin, P. (2014) Toehold switches: de-novo-designed regulators of gene expression. *Cell* 159 (4), 925–939.
- (32) Yurke, B., Turberfield, A. J., Mills, A. P., Jr., Simmel, F. C., and Neumann, J. L. (2000) A DNA-fuelled molecular machine made of DNA. *Nature* 406 (6796), 605.
- (33) Dirks, R. M., and Pierce, N. A. (2004) Triggered amplification by hybridization chain reaction. *Proc. Natl. Acad. Sci. U. S. A.* 101 (43), 15275–15278.
- (34) Pardee, K., Slomovic, S., Nguyen, P. Q., Lee, J. W., Donghia, N., Burrill, D., Ferrante, T., McSorley, F. R., Furuta, Y., and Vernet, A. (2016) Portable, on-demand biomolecular manufacturing. *Cell* 167 (1), 248–259.
- (35) Pardee, K., Green, A. A., Ferrante, T., Cameron, D. E., DaleyKeyser, A., Yin, P., and Collins, J. J. (2014) Paper based synthetic gene networks. *Cell* 159 (4), 940–954.
- (36) Xie, F., Ling, L., van Dam, H., Zhou, F., and Zhang, L. (2018) TGF- $\beta$  signaling in cancer metastasis. *Acta Biochim. Biophys. Sin.* 50 (1), 121–132.
- (37) Guo, L., Zhang, Y., Zhang, L., Huang, F., Li, J., and Wang, S. (2016) MicroRNAs, TGF- $\beta$  signaling, and the inflammatory microenvironment in cancer. *Tumor Biol.* 37 (1), 115–125.
- (38) Suzuki, H. (2018) MicroRNA Control of TGF- $\beta$  Signaling. *Int. J. Mol. Sci.* 19 (7), 1901.
- (39) Luo, K. (2017) Signaling cross talk between TGF- $\beta$ /Smad and other signaling pathways. *Cold Spring Harbor Perspect. Biol.* 9 (1), a022137.